Accepted Manuscript
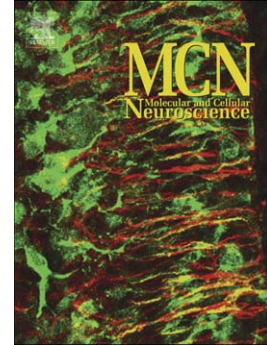
PACAP/PAC$_1$R signaling modulates acetylcholine release at neuronal nicotinic synapses

Phyllis C. Pugh, Selwyn S. Jayakar, Joseph F. Margiotta

Please cite this article as: Pugh, Phyllis C., Jayakar, Selwyn S., Margiotta, Joseph F., PACAP/PAC$_1$R signaling modulates acetylcholine release at neuronal nicotinic synapses, *Molecular and Cellular Neuroscience* (2009), doi:10.1016/j.mcn.2009.11.007

Title: PACAP/PAC$_1$R signaling modulates acetylcholine release at neuronal nicotinic synapses.

Authors: Phyllis C. Pugh, Selwyn S. Jayakar, and Joseph F. Margiotta

Project Address: University of Toledo College of Medicine, Department of Neurosciences

Block HS 108, 3000 Arlington Ave., Mail Stop #1007, Toledo, OH 43614-5804.

Affiliations: Joseph F. Margiotta, Ph.D. (Corresponding Author)

University of Toledo College of Medicine, Department of Neurosciences

Mail Stop #1007, Block HS 108, 3000 Arlington Ave., Toledo, OH 43614-5804

Tel: 419-383-4119; Fax: 419-383-3008; E-mail: joseph.margiotta@utoledo.edu

Phyllis C. Pugh, Ph.D., University of Alabama, Dept. of Neurobiology, Birmingham, AL 35294

Selwyn S. Jayakar, Ph.D., University of Toledo College of Medicine, Department of Neurosciences, Toledo, OH 43614-5804

Dedication: This paper is dedicated to the memory of Desiree Pardi MD/PhD who pioneered studies of PACAP in this laboratory for her PhD thesis research. Desiree died peacefully on September 6, 2009.

1

ABSTRACT

Neuropeptides collaborate with conventional neurotransmitters to regulate synaptic output. Pituitary adenylate cyclase-activating polypeptide (PACAP) co-localizes with acetylcholine in presynaptic nerve terminals, is released by stimulation, and enhances nicotinic acetylcholine receptor-(nAChR-) mediated responses. Such findings implicate PACAP in modulating nicotinic neurotransmission, but relevant synaptic mechanisms have not been explored. We show here that PACAP acts *via* selective high-affinity G-protein coupled receptors (PAC$_1$Rs) to enhance transmission at nicotinic synapses on parasympathetic ciliary ganglion (CG) neurons by rapidly and persistently increasing the frequency and amplitude of spontaneous, impulse-dependent nicotinic excitatory postsynaptic currents (sEPSCs). Of the canonical adenylate cyclase (AC) and phospholipase-C (PLC) transduction cascades stimulated by PACAP/PAC$_1$R signaling, only AC-generated signals are critical for synaptic modulation since the increases in sEPSC frequency and amplitude were mimicked by 8-Bromo-cAMP, blocked by inhibiting AC or cAMP-dependent protein kinase (PKA), and unaffected by inhibiting PLC. Despite its ability to increase agonist-induced nAChR currents, PACAP failed to influence nAChR-mediated impulse-independent miniature EPSC amplitudes (quantal size). Instead, evoked transmission assays reveal that PACAP/PAC$_1$R signaling increased quantal content, indicating it modulates synaptic function by increasing vesicular ACh release from presynaptic terminals. Lastly, signals generated by the retrograde messenger, nitric oxide- (NO-) are critical for the synaptic modulation since the PACAP-induced increases in spontaneous EPSC frequency, amplitude and quantal content were mimicked by NO donor and absent after inhibiting NO synthase (NOS). These results indicate that PACAP/PAC$_1$R activation recruits AC-dependent signaling that stimulates NOS to increase NO production and control presynaptic transmitter output at neuronal nicotinic synapses.

INTRODUCTION

Neuropeptides activate specific cell-surface receptors, triggering intracellular signals that regulate an array of cellular functions. Pituitary adenylate-cyclase activating polypeptide (PACAP) is a 38 amino acid neuropeptide first isolated from ovine hypothalamus and now known to be widely expressed throughout the nervous system (Miyata et al., 1989; Hannibal, 2002). PACAP modulates the function of ion channels and synaptic components, provides neuroprotective and neurotrophic support, and potently alters neuronal gene expression (Vaudry et al., 2000; Sumner and Margiotta, 2008). In parasympathetic ciliary ganglion (CG) neurons, PACAP acts *via* selective, high-affinity, G-protein coupled receptors (PAC$_1$Rs) that activate both adenylate cyclase- (AC-) and phospholipase-C- (PLC-) dependent transduction cascades (Margiotta and Pardi, 1995; Pardi and Margiotta, 1999). The resultant signaling rapidly regulates both heteromeric nicotinic ACh receptors (containing $\alpha3$, $\alpha5$, $\beta4$, $\pm$ $\beta2$ subunits; $\alpha3^*$-nAChRs) and homomeric $\alpha7$-nAChRs, and mobilizes intracellular calcium (Margiotta and Pardi, 1995; Pardi and Margiotta, 1999; Woo and Margiotta, 2007). Over the long term, PACAP-generates activity- and AC-dependent signals that support neuronal survival by blunting apoptosis (Pugh and Margiotta, 2006). Recent studies indicate PACAP/PAC$_1$R signaling also induces time-dependent alterations in gene expression related to development and synaptic function in both sympathetic (Girard et al., 2004; Braas et al., 2007) and CG neurons (Sumner and Margiotta, 2008). Interestingly, PACAP co-localizes with ACh in presynaptic nerve terminals in adrenal gland, sympathetic, and ciliary ganglia (Hamelink et al., 2002; Ermilov et al., 2004; Sumner et al., 2004). Taken together, these findings highlight PACAP's pleiotropic actions, and suggest its activity- and time-dependent influences on local neuron targets *in vivo* involve regulation of synaptic function.

The expectation that PACAP would regulate the function of neuronal nicotinic synapses was tested in the present experiments. Evidence for activity-dependent PACAP release was obtained by showing that PACAP immunoreactivity disappears from presynaptic cholinergic terminals in the CG after treatment with depolarizing $[K^+]_{out}$. To determine its influence on nicotinic synapses, PACAP was applied to CG cultures where the neurons recapitulate key developmental milestones, including morphological specialization, expression of nAChRs, and elaboration of nicotinic synapses that mimic

4

their counterparts *in vivo* (Ravdin and Berg, 1979; Margiotta and Berg, 1982; Role and Fischbach, 1987; Chen et al., 2001). PACAP dramatically enhanced spontaneous synaptic activity in the cultures, increasing the average frequency and amplitude of spontaneous, impulse-dependent excitatory postsynaptic currents (sEPSCs) recorded from CG neurons within minutes. The PACAP-induced changes in synaptic function required PAC_1R signaling *via* AC and PKA. Measurements of repetitive spike firing characteristics, and analysis of quantal EPSC components reveal that PACAP enhanced synaptic activity neither by increasing excitability nor by upregulating postsynaptic nAChRs (quantal size) but did so by increasing vesicular ACh release (quantal content) from presynaptic terminals. Further, the PACAP-induced increase in quantal content required activation of the gaseous messenger, nitric oxide (NO). These results are consistent with the pleiotropic actions of PACAP, and reveal an unexpected relevance for PACAP/PAC_1R signaling *via* NO to regulate ACh release from presynaptic terminals at neuronal nicotinic synapses.

METHODS

Cell Culture. Neuronal cultures were prepared from embryonic day 8 (E8) ciliary ganglia as previously described (Chen et al., 2001). Briefly, ganglia were treated with trypsin (0.025%, 15 min, 37°C) and CG neurons dispersed by trituration and grown on coated glass coverslips. The growth medium consisted of Eagle's minimum essential medium supplemented with 2 mM glutamine, 100 U/ml penicillin, 100 μg/ml streptomycin, and 10% heat-inactivated horse serum (MEM, all components from Invitrogen, Rockville, MD) and with freshly-prepared E17 chick eye extract (3% v/v, MEM/eye). Glass coverslips (#1, 12 mm, Fisher Scientific) were acid-washed and coated with 0.2 mg/ml poly-D-ornithine and 30 ng/ml mouse laminin (Collaborative Biomedical, Bedford, MA). Coverslip cultures were maintained for up to 7 d in 16 mm multiwell plates at 37°C in 95% air and 5% CO_2, and the culture medium replenished every 2-3 d.

Microscopy. To localize PACAP and assess its depletion, E19 ciliary ganglia were incubated (30 min, 22°C) in MEM containing normal (5 mM) or depolarizing (50 mM) KCl, and then processed using a whole ganglion imaging protocol (Rubio et al., 2005) modified to accommodate PACAP signal amplification {Tyramide signal amplification (TSA) kit, Molecular Probes/Invitrogen, Carlsbad, CA}. Control and KCl-treated ganglia were fixed with 4% paraformaldehyde freshly prepared in 0.1 M Phosphate buffered saline (PBS, 30 min, 22°C), washed in PBS (16h, 4°C), and incubated in PBS containing 3% H_2O_2 (1h, 22°C) to quench endogenous peroxidase activity. Ganglia were then incubated (16h, 4°C) in block solution (PBS containing 0.1% Triton X-100, and 1% TSA kit block reagent) with Avidin D (150 μl/ml; Avidin/Biotin Blocking Kit; Vector Laboratories, Burlingame, CA) added to mask endogenous biotin. Ganglia were washed in PBS and incubated with antibodies recognizing the presynaptic marker Synapsin-I (pAb1543, 1:250, Chemicon/Millipore, Billerica, MA) and PACAP-38 (mAbJHH1, 1:100, provided by Jens Hannibal, University of Copenhagen) in block solution containing 150 μl/ml Biotin (16h, 4°C). Next, ganglia were washed in PBS, and Synapsin-I and PACAP labeling were detected using Alexa Fluor 488-conjugated goat anti-rabbit IgG (Molecular Probes/Invitrogen, Carlsbad, CA) and biotinylated goat anti-mouse IgG (Kirkegaard Perry Laboratories, Gaithersburg, MD), respectively (both at 1:200 in block solution lacking Triton X-100, 16 h, 4°C). To amplify the

6

PACAP signal, ganglia were washed in PBS, incubated in Triton-free block solution containing horseradish peroxidase-conjugated streptavidin (1:100, TSA kit, 1h, 22°C), washed, incubated in amplification buffer with 0.0015% H_2O_2 and Alexa Fluor 546-labeled tyramide (1:100, TSA kit, 10 min, 22°C). Ganglia were washed again, mounted in Vectashield (Vector Laboratories; Burlingame, CA) and examined using an Olympus BX51 microscope equipped with a 1.2 NA 60X objective, and a BioRad Radiance2000 laser scanning confocal system (Carl Zeiss MicroImaging, Thornwood, NY). Optical Z-sections were acquired sequentially through the ganglia in 1.0 μm steps using BioRad Lasersharp software, with power and gain settings that minimized pixel saturation and produced no detectable bleed-through between Ar (488 nm) and Green HeNe (543 nm) laser channels. Images were analyzed using ImageJ (v1.40g) (Rasband, 2004) plugins to evaluate signal intensities and colocalization (by Mander's coefficients, M).

Electrophysiology. After 5 d in culture, recordings were obtained from CG neurons bathed at 22°C in a recording solution containing (in mM): 145 NaCl, 5.3 KCl, 5 HEPES, 5.4 Glucose, 0.8 $MgSO_4$, 2 $CaCl_2$ (RS) supplemented with 10% heat inactivated horse-serum (RS^{hs}; pH 7.4). Patch pipettes (2-4 MΩ) were fabricated from Corning 8161 glass tubing and filled with (in mM) 145.6 CsCl, 0.6 $CaCl_2$, 2.0 EGTA, 15.4 glucose, and 5.0 Na-HEPES (pH 7.3). In most experiments, membrane currents were acquired from neuron somas in the whole-cell configuration using Axopatch 1B or 200B patch clamps (Molecular Devices, Sunnyvale, CA) and digitized, usually at 100 μs intervals, using an ITC-16 interface and Pulse 8.6.3 software (InstruTECH/HEKA, Bellmore, NY) controlled from a Macintosh G4 computer running OS-9. The standard holding potential (V_{hold}) was -70 mV, and neurons typically had input resistances >500 MΩ; those displaying peak voltage-activated Na^+ currents <150 pA/pF (150 pA/pF X 20 pF = 3000 pA) were excluded.

Synaptic function was assessed by analyzing both spontaneous and stimulus-evoked EPSCs. Spontaneously arising EPSCs (sEPSCs) were acquired without stimulation, as previously described (Chen et al., 2001). In other experiments, EPSCs were evoked (eEPSCs) by applying *"en-passant"* stimuli to neurite fasicles converging on individual CG neuron somas held in whole-cell mode. To do so,

bipolar electrodes were fabricated from theta-glass capillary tubing (TG150-4, Warner Instruments, Hamden, CT) pulled to 1-3 µm overall diameter, the barrels filled with RS, and the electrode mounted in a ported theta-glass holder (THS-F15PH, Warner Instruments, Hamden, CT) connected to an isolated stimulator (Model 2100, A-M Systems, Carlsborg, WA). Neurite fasicles were isolated by partially drawing them into the electrode barrels using gentle suction, and voltage pulses (100-300 µsec) applied between the barrels. The stimulus intensity was adjusted to activate single axons, as determined by "minimal stimulation" criteria (e.g., further reducing stimulus intensity elicited eEPSCs in the follower neuron less than 25% of the time). We considered the criteria satisfied when stimuli were just sufficient to evoke EPSCs that (1) activated with brief constant delay, (2) activated to full amplitude without notches indicative of a secondary component, and (3) had amplitudes and kinetics matching those of sEPSCs in the same culture. Miniature EPSCs (mEPSCs) were obtained either from spontaneous synaptic events acquired while blocking Na^+ channel dependent action potentials with tetrodotoxin (TTX, 1 µM; i_s), or from unitary synaptic events isolated from amplitude histograms collected in evoked transmission assays (i_e).

Spontaneous sEPSCs and mEPSCs were examined off-line using Mini Analysis (6.0.3, Synaptsoft, Fort Lee, NJ) as previously described (Chen et al., 2001; Zhou et al., 2004). Only those events that arose abruptly and had peak amplitudes >2.5 X baseline RMS current noise (typically 1-2 pA) were selected for analysis. For each neuron, the timing and peak size of selected events were exported to Excel spreadsheets (11.5.5, Microsoft, Redmond, WA). Average sEPSC and mEPSC frequencies (F_s and f_s, Hz) were determined from the total number of events divided by the recording epoch duration (usually 2 min) while sEPSC and mEPSC amplitudes were characterized from the average of individual amplitudes (I_s and i_s, pA). To examine the distribution of EPSC frequencies and amplitudes, F_s, f_s, I_s, and i_s values were compiled in cumulative histograms using Prism (4.0a, GraphPad, La Jolla, CA). Stimulus-evoked EPSCs were identified using PulseFit (8.66, HEKA Instruments, Bellmore, NY) using the minimal stimulation and detection criteria described above, with the added requirement that they occur with fixed synaptic delay following fasicle stimulation. While the total delay was stable for any given trial, it varied between trials (typically from ≈2-10 ms) likely because the distance between stimulating electrode and soma recording patch pipette ranged from ≈20-100 µm.

8

For each recording, average eEPSC amplitudes (I_e) were determined from the sum of all event amplitudes (including failures, I_e = 0) divided by the total number of applied stimuli (usually 120). Unitary, mEPSC amplitudes (i_e) were obtained by averaging event amplitudes within in the lowest component size of histograms assembled from all evoked events.

The plasma membrane nAChR population was stimulated by focally applying nicotine (Nic, 20 µM in RS) *via* microperfusion (7-10 psi) to CG neuron somas held at -70 mV. To ensure selective α3*-nAChR activation, the cultures were pretreated with 50 nM αBgt to block α7-nAChR for 1h as previously described (Nai et al., 2003; Zhou et al., 2004). The resulting peak current amplitudes and slow current decay were analyzed using Clampfit (pClamp 6.0 or 8.0, Axon Instruments, Burlingame, CA) as previously described (Nai et al., 2003; Zhou et al., 2004). Peak response amplitudes were normalized to neuron soma membrane capacitance (pA/pF), and values obtained from PACAP-treated (100 nM, 15 min) and control neurons from the same cultures compared. Tetrodotoxin (TTX, 1 µM) was included in some experiments to test the effect of action potential blockade.

To assess changes in membrane excitability associated with PACAP treatment (Braas et al., 1998; DeHaven and Cuevas, 2004), patch pipettes were filled with 110 KMeSO$_4$, 10 NaCl, 5 MgCl$_2$, 0.6 EGTA, and 10 HEPES and the recording mode switched from voltage- to current-clamp after attaining the whole-cell configuration. Neurons displaying resting potential (V_{rest}) values >-40 mV or input resistance (R_{in}) values <500 MΩ were excluded. A family of 200 ms depolarizing current pulses (from 6 to 96 pA, in 6 pA steps) was applied at 0.1 Hz to initiate action potentials. Action potential numbers and inter-spike intervals were computed and analyzed as a function of the applied current for PACAP-treated and control neurons.

Drug treatments. Unless otherwise stated, all reagents were added directly to established cultures maintained in MEM/eye. Acute treatments were for 15 min prior to recording on d 5 in culture. For washout studies, the media was replaced with MEM/eye at the end of treatment (for an additional 30 min to 48 h). When signaling pathway inhibitors were tested, the neurons were pre-treated with the inhibitor for 15 min prior to exposure to PACAP (total treatment time of 30 min). Treatment conditions included elevated KCl (addition of 45 mM KCl), PACAP38 (1-300 nM; American Peptide, Inc.,

Sunnyvale, CA), forskolin (10 µM), 8-Bromo-cyclic AMP (8Br-cAMP, 2 mM), SQ22536 (10-100 µM), MDL12330A (1-100 µM), H89 (10 µM), U73122 (0.1-1.0 µM), Myr-GRTGRRNAI-NH$_2$ [PKI(14-22), 1 µM, Myristoylated Protein Kinase A Inhibitor Amide 14-22, EMD Biosciences, San Diego, CA], L-Nitro-Arginine Methyl Ester (L-NAME, 100 µM), and sodium nitroprusside (SNP, 100 µM), either alone or in combinations, as described. Both maxadilan and Max.d.4 (PAC$_1$ agonist and antagonist, respectively) (Moro and Lerner, 1997; Moro et al., 1999) were generously provided by E. A. Lerner (Massachusetts General Hospital, Charlestown, MA). Unless otherwise specified, the pharmacological agents were purchased from Sigma-Aldrich (St. Louis, MO). The concentrations of activators and inhibitors used were based on previous studies either by this lab or others (Margiotta and Pardi, 1995; Csernus et al., 1999; Gadea et al., 1999; McIntosh et al., 1999; Pardi and Margiotta, 1999; Kimura, 2000; Pugh and Margiotta, 2000; Kanda and Watanabe, 2001; Mohamed et al., 2001; Wang et al., 2004; Zhou et al., 2004; Pugh and Margiotta, 2006).

Statistics. Parameter values (i.e. F_s, f_s, I_s, I_e, i_s, and i_e) are expressed as mean ± SEM followed by the number of neurons from which values were obtained (n). Values from test conditions normalized to averages from control neurons in the same experiments are indicated by asterisks (e.g. F_s*, I_s*, etc). The statistical significance of differences in parameter values between control and PACAP treatment groups was determined using Student's unpaired, two-tailed *t*-test (*t*-test, $p < 0.05$) with Welch's correction for unequal variances used as necessary (Prism 4.0a). For comparisons of multiple treatment groups, significance was determined by one way ANOVA followed by Bonferroni's multiple comparison *post-hoc* test ($p < 0.05$; Prism 4.0a). Differences in parameter value cumulative distributions were assessed using the Kolmogorov-Smirnov (KS) test ($p < 0.05$, available online at http://www.physics.csbsju.edu/stats/KS-test.html).

RESULTS

PACAP localization and release. To test PACAP's potential for modulating nicotinic transmission, we first assessed its localization and voltage-dependent release *in situ*. In the developing CG, ciliary neurons receive 1:1 cholinergic input from accessory occulomotor neuron axons that terminate in a distinctive calyx enveloping most of the postsynaptic neuron surface (Hess, 1965; Landmesser and Pilar, 1972; Cantino and Mugnaini, 1975; Paysan et al., 2000). Consistent with their role as presynaptic terminals, calyces are strongly immunoreactive for the presynaptic markers, SV2 (Wilson Horch and Sargent, 1995) and Synapsin I. Further, Synapsin I and PACAP immunolabeling overlap considerably (Fig. 1A-C; $M_{S:P} \approx M_{P:S} \approx 0.70$), confirming that PACAP colocalizes with ACh in presynaptic terminals within the CG (Sumner et al., 2004). Previous studies have shown that neurotransmission from calyx to ciliary neuron reliably follows stimuli delivered at frequencies up to 50 Hz (Dryer and Chiappinelli, 1985) and that 16-20 Hz stimulation is sufficient to trigger PACAP release from splanchnic nerve terminals and intercardiac nerve fibers (Tornoe et al., 2000; Lamouche and Yamaguchi, 2001; Tompkins et al., 2007) where it is a co-transmitter with ACh (Hamelink et al., 2002; Tompkins et al., 2007). Consistent with activity-dependent PACAP release in the CG, sustained depolarization achieved by treating ciliary ganglia with RS containing 50 mM KCl (15 min) abolished PACAP immunolabeling in calyces (Fig. 1D-F; $M_{S:P} \approx 0.02$), leaving Synapsin I immunolabeling unaffected. Together with its ability to enhance nAChR function (Margiotta and Pardi, 1995; Pardi and Margiotta, 1999) and regulate catecholamine secretion (Hamelink et al., 2002), PACAP's localization in and activity-dependent release from cholinergic terminals prompted us to examine its functional role in modulating nicotinic neurotransmission.

PACAP increases EPSC frequency and amplitude at nicotinic synapses on CG neurons. CG neurons form an extensive synaptic network in culture, and by 3 d nearly all display sEPSCs (Margiotta and Berg, 1982; Chen et al., 2001). The vast majority of sEPSCs are mediated by $\alpha3^*$-nAChRs since treating cultures with αCTx-MII to block $\alpha3^*$-nAChRs (Chen et al., 2001) drastically reduced both sEPSC frequency and amplitude, while blocking $\alpha7$-nAChRs with αBgt had little effect (Chen et al., 2001). In the present studies, sEPSCs recorded from control cultures occurred at frequencies of 0.4 -

11

2.0 Hz and displayed peak amplitudes of 6 - 100 pA with overall mean values (F_s and I_s) of 1.3 ± 0.1 Hz and 14.6 ± 0.4 pA, respectively (n = 262 neurons from 59 experiments). After 15 min application of 100 nM PACAP, overall synaptic activity increased (Fig. 2A), as was reflected in F_s and I_s shifts to significantly larger mean values (2.5 ± 0.2 Hz and 18.6 ± 0.6 pA, respectively; n = 146) that were 3.8- (F_s*) and 1.4- (I_s*) times those obtained from sham-treated control neurons (n = 154) tested in the same experiments (Fig. 2B, C). In time course studies, PACAP was seen to induce maximal increases in F_s* and I_s* within 5 min, and its effects were sustained for up to 48 h following a single brief application (Fig. 2D, E). Thus PACAP rapidly increases both nicotinic sEPSC frequency and amplitude, and the synaptic modulation persists long after its removal.

PACAP modulates nicotinic synapses via PAC₁Rs and AC/PKA-mediated signal transduction.

PACAP activates two related classes of G-protein coupled receptors. VPAC receptors (VPACRs) have high affinity for both vasoactive intestinal peptide (VIP) and PACAP (K_D ≈1 nM), while PAC_1Rs are PACAP-selective, having up to 1000-fold lower affinity for VIP (K_D ≈1 μM) (Vaudry et al., 2000). CG neurons express abundant PAC_1Rs. Previous competition studies indicated high-affinity PACAP binding on intact CG neurons, showing that peptide concentrations required to inhibit [125]-I-PACAP binding to half-maximum (IC_{50}) were 2000-fold lower for PACAP (0.5 nM) than for VIP (1 μM) (Margiotta and Pardi, 1995). PAC_1Rs signal *via* two canonical transduction cascades; one requiring PLC, inositol phosphate (IP) production and $[Ca^{2+}]_{in}$ mobilization, and another requiring AC, cAMP production and subsequent PKA phosphorylation of downstream target proteins (Rawlings, 1994). In accord with the presence of signaling competent PAC_1Rs (Vaudry et al., 2000) PACAP is >10-fold more potent than VIP in stimulating both cAMP production and IP turnover in CG neurons (Margiotta and Pardi, 1995; Pardi and Margiotta, 1999). While recent PCR experiments reveal transcripts encoding VPACR and PAC_1R isoforms in CG RNA (Sumner, Pugh, and Margiotta, unpublished) only PAC_1Rs that couple *via* AC/PKA-mediated transduction were required to enhance synaptic function. *First*, consistent with PAC_1R involvement, PACAP potently and selectively enhanced synaptic function (Fig. 3A). Increasing PACAP concentrations (1-100 nM) produced progressively larger values of sEPSC F_s and I_s, and the nanomolar concentrations required to produce half-maximal stimulation (EC_{50} ≈ 5 nM for both) were indicative of high potency. In accord with PACAP-selective actions, VIP failed to significantly augment

either F_s or I_s when applied at 100 nM, a concentration at which PACAP produces maximal effects. *Second,* although PACAP potently activates PLC- as well as AC-dependent transduction in CG neurons (Margiotta and Pardi, 1995; Pardi and Margiotta, 1999) only AC-dependent signaling was necessary to modulate nicotinic synaptic function (Fig. 3B, C). Specifically, the ability of PACAP to increase sEPSC F_s and I_s was unaffected by inhibiting PLC with U-73122, previously shown to block PACAP stimulated IP turnover and $[Ca^{2+}]_{in}$ mobilization in CG neurons (Pardi and Margiotta, 1999). Consistent with this finding, treatment with muscarine (100 µM) which activates muscarinic acetylcholine receptors and induces IP turnover in the neurons (Rathouz et al., 1995) failed to enhance sEPSC F_s and I_s. By contrast, PACAP-induced increases in F_s and I_s were blocked by inhibiting AC with either MDL12330A (Guellan et al., 1977) or SQ-22356, a reagent previously shown to reduce cAMP production in CG neurons by ≈80% (Margiotta and Pardi, 1995). Consistent with AC-mediated transduction, the PACAP-induced enhancement of sEPSC F_s and I_s was mimicked by 8Br-cAMP, a membrane permeable cAMP analogue previously shown to enhance nAChR responses similar to that of PACAP (Margiotta et al., 1987; Margiotta and Pardi, 1995). Further supporting a requirement for AC- and cAMP-mediated signaling, PACAP's actions on sEPSCs were also blocked by PKI(14-22), a specific PKA inhibitor (Glass et al., 1989). This last finding indicates that, like PACAP-induced neuronal survival and nAChR upregulation (Pardi and Margiotta, 1999; Pugh and Margiotta, 2006), synaptic modulation is based on canonical AC signaling requiring cAMP accumulation and PKA phosphorylation of downstream targets. Taken together these relative-potency and effector-dependence experiments indicate that PACAP engages PAC$_1$Rs that efficiently couple to AC/PKA-mediated transduction to modulate synaptic function.

PACAP does not increase the excitability of CG neurons. We considered three possible mechanisms whereby PACAP/PAC$_1$R signaling could enhance sEPSC F_s and I_s. The first was by increasing neuronal excitability, as was found in previous studies where PACAP markedly increased action potential repetitive firing in cardiac ganglion neurons by ≈5-fold, concomitant with a sustained (≈5-7 mV) depolarization (Braas et al., 1998; DeHaven and Cuevas, 2004; Tompkins et al., 2007). PACAP (100 nM) did depolarize CG neurons since resting potentials recorded in current-clamp mode after 5 to 15 min treatments were -48.1 ± 0.8 mV (n = 8) compared with -53.9 ± 0.4 mV (n = 8) for

13

sham-treated neurons from the same cultures tested in parallel ($p < 0.05$, *t*-test). The latter values were indistinguishable from the -56.0 ± 1.0 mV mean resting potentials ($p > 0.05$, n = 80, *t*-test) previously obtained from CG neurons in culture using sharp electrodes (Margiotta and Berg, 1982). Unlike cardiac ganglion neurons, however, PACAP markedly reduced the excitability of CG neurons. As depicted in Fig. 4, control CG neurons fired low-frequency action potentials when sufficiently depolarized such that the number of spikes increased linearly from 1.4 at 6 pA to 4.5 at 96 pA (slope = 0.039 pA^{-1}). After PACAP treatment, however, repetitive firing was virtually abolished with only 1.0-1.8 spikes elicited over the same stimulus range (slope ≈ 0.001 pA^{-1}). In addition, the membrane potential threshold required to produce an action potential was more depolarized in the PACAP-treated neurons (-43.9 ± 1.1 mV, n = 8) relative to that for controls (-49.0 ± 0.3 mV, n = 8, $p < 0.05$) and the net voltage from baseline to action potential peak (ΔV) was significantly decreased after PACAP treatment (from ΔV = 79.2 ± 3.1 mV to 63.2 ± 3.5 mV, for control and PACAP-treated neurons, n = 7 and 5 cells, respectively). Lastly, in cases where PACAP treated neurons displayed >1 action potential, the increase in spike frequency as a function of stimulus strength was indistinguishable from that of control neurons (slope ≈ 0.2 Hz/pA for both, p > 0.2, *F*-test; data not shown). Mechanisms underlying these PACAP-induced changes in membrane properties were not examined further. Nevertheless, the higher action potential threshold and depressed action potential firing are inconsistent with what would be expected if PACAP enhanced synaptic function by increasing the excitability of CG neurons.

PACAP does not alter postsynaptic AChRs. The remaining candidate mechanisms for the enhanced synaptic function involve PACAP influencing either postsynaptic nAChRs or presynaptic ACh release and were addressed by analyzing quantal components of spontaneous and evoked EPSCs. Since PACAP increases sEPSC amplitude (I_s, Fig. 2) and previous rapid agonist application studies revealed that it rapidly increases α3*-nAChR responses from acutely dissociated E14 CG neuron somas (Margiotta and Pardi, 1995; Pardi and Margiotta, 1999) tests for a postsynaptic mechanism were conducted first. mEPSCs are considered indicative of nAChRs activated at postsynaptic clusters by ACh released from single vesicles from adjacent presynaptic terminals (Lin and Bennett, 1994; Bekkers and Stevens, 1995; Chen et al., 2001; Conroy et al., 2007). If PACAP enhanced transmission by a mechanism involving global upregulation of all α3*-nAChRs on the neuron soma, including those at

14

postsynaptic sites, it would be expected to increase average mEPSC amplitude (i_s, quantal size) since we previously found that the vast majority of sEPSCs are sensitive to blockade by αCTx-MII and hence mediated by α3*-nAChRs (Chen et al., 2001; Nai et al., 2003). Quantal, nAChR-mediated mEPSCs are detectable in CG neurons following action potential blockade with TTX (1 μM) and are smaller and occur at lower frequencies than impulse-dependent sEPSCs both *in situ* and in culture (Scott and Bennett, 1993a; Scott and Bennett, 1993b; Lin and Bennett, 1994; Ullian et al., 1997; Chen et al., 2001). In the present experiments, criterion mEPSCs (i.e. events with peak amplitudes at least 2.5 X baseline RMS current noise) were routinely observed after TTX treatment (Fig. 5). The mEPSCs were quite uniform in size, since the vast majority had amplitudes that fell within one standard deviation of the overall mean value (i_s = 7.2 ± 0.3 pA; n = 37) both within and across a total of nine separate cultures (Fig. 5A and B). In addition, and as expected for quantal events, mEPSC frequency and amplitude were independent of $[Ca^{2+}]_{out}$ ranging from 0 to 5 mM (data not shown). Moreover, treating cultures with αBgt (50 nM, 1 h) to block α7-nAChRs, the only other nAChR subtype expressed by the neurons (Nai et al., 2003) failed to alter either mEPSC frequency or amplitude, respectively (0.59 ± 0.14 Hz and 7.6 ± 0.5 pA, n = 4), relative to untreated controls (0.70 ± 0.47 Hz and 6.5 ± 1.4 pA, n = 3) from the same experiments (p > 0.5 for both, *t*-test). These and previous pharmacological tests with αCTx-MII indicate that the vast majority of detectable mEPSCs are mediated by the α3*-nAChR subtype. To our surprise, mEPSCs acquired from PACAP/TTX-treated neurons were very similar to those acquired from neurons treated with TTX alone and tested in the same four experiments (Fig. 5B-D, Table 1). A shift to slightly higher maximal mEPSC frequencies was evident in cumulative distributions compiled for PACAP/TTX treated neurons relative to accompanying TTX-controls, but the mean f_s value for these treated neurons was not measurably different from that for TTX-controls. Moreover, mEPSC amplitudes were not detectably influenced by PACAP since neither the cumulative distributions nor the mean i_s values for PACAP/TTX-treated and TTX-control neurons differed significantly.

We first examined whether the failure of PACAP to influence mEPSC amplitude resulted from a paradoxical failure of PACAP/PAC$_1$R signaling to influence synaptic function. When tested in these same experiments, however, PACAP treated, TTX-naïve neurons (n = 16) displayed F_s and I_s values that were 4.0 ± 0.7 times and 1.8 ± 0.2 times those of corresponding values obtained from TTX-naïve

neurons (n = 22) tested in parallel ($p < 0.05$ for both F_s and I_s, t-test). We next addressed the possibility that the recording setup was insufficiently sensitive to resolve 25-75% increases in quantal size necessary to account for the increase in I_s. This possibility was also rejected because after changing the holding potential from -70 to -90 mV a predictable 30% increase in mEPSC amplitude was easily resolved (data not shown). Lastly, we considered that α3*-nAChR upregulation by PACAP may not occur in culture, particularly after treatment with TTX. This possibility was also eliminated since peak whole-cell α3*-nAChR current amplitudes induced by rapid nicotine microperfusion in PACAP treated neurons were ≈2.4 times larger than those of sham-treated controls, and a similar enhancement was observed when incubations and tests were conducted in the presence of TTX (Fig. 5E). These experiments indicate that while PACAP/PAC$_1$R signaling rapidly increases α3*-nAChR-mediated currents in CG neurons, it fails to influence quantal size. Thus postsynaptic α3*-nAChRs, responsible for the vast majority of sEPSCs and mEPSCs seen previously and here appear refractory to further regulation by exogenous PACAP.

PACAP enhances synaptic activity by increasing mean quantal content. Having rejected postsynaptic nAChRs as targets of PACAP/PAC$_1$R signaling relevant to synaptic modulation, we addressed the possibility that PACAP alters presynaptic function. To do so, altered ACh release was evaluated by measuring mean quantal content (*m*) presumed to represent the average number of presynaptic vesicles released by a single impulse (Johnston and Wu, 1995). Initial determinations of *m* were based on sEPSCs and obtained from average sEPSC and mEPSC amplitudes (I_s and i_s) using the empirical relation $m_s = I_s/i_s$ (del Castillo and Katz, 1954; Johnston and Wu, 1995). When calculated using I_s and i_s values obtained from separate neurons from the same cultures, m_s (2.0 ± 0.3, n =19, Table 1) was indistinguishable from that calculated using I_s and i_s values compiled from individual neurons before and after TTX treatment (m_s = 1.6 ± 0.1, n = 3; $p > 0.5$, t-test). Using the former method we calculated that PACAP treatment increased m_s to ≈1.6 times that of sham treated controls from the same experiments (2.9 ± 0.3, n = 16; $p < 0.01$, Table 1). While this finding suggests that PACAP enhances nicotinic synaptic transmission by influencing presynaptic function, sEPSC-based determinations of quantal content are potentially limited by two opposing factors. *First*, impulse independent mEPSCs will be included, skewing the distribution of sEPSC amplitudes to lower values

16

and reducing m. *Second*, transmission failures (where $I_s = 0$) will be unresolved and thus not included in the overall averages, as would be appropriate (del Castillo and Katz, 1954; Johnston and Wu, 1995), skewing overall sEPSC amplitudes to higher values and increasing m.

To circumvent these potential problems, we devised a way to evoke transmission between pre- and postsynaptic neuron pairs. In doing so, it was presumed that any given neuron would most likely receive direct presynaptic input from axons traveling in neurite fasicles that converge upon its soma. Indeed, when convergent fasicles were stimulated, short-latency currents indicative of synaptic transmission evoked by single axon impulses were seen in ≈90% of target somas (n = 58 fasicles, 25 neurons), whereas stimulation of non-convergent fasicles failed to evoke such currents (Fig. 6A). The currents induced by convergent fasicle stimulation met criteria expected for impulse-dependent, nAChR-mediated evoked EPSCs (eEPSCs). They arose with fixed delay, their brief onset and slower decay kinetics resembled those of $\alpha 3^*$-nAChR-mediated sEPSCs (Fig. 6A,B), their peak amplitudes were increased by hyperpolarization and reduced by depolarization, and they were reversibly abolished by blocking Na$^+$ channels with TTX or nAChRs with *d*-tubocurarine (data not shown).

The ability to reliably evoke transmission between CG neuron pairs allowed us to test two established methods for evaluating quantal components of transmission at individual synapses (Martin and Pilar, 1964; Johnston and Wu, 1995). The first is empirical where m_e is based on the ratio of average evoked response amplitudes (I_e, including failures where $I_e = 0$) relative to average unitary mEPSC amplitudes (i_e) collected from the same neurons ($m_e = I_e/i_e$). Importantly, i_e values differed from those of spontaneous event amplitudes acquired in TTX (i_s) by <15%, and PACAP treatment similarly failed to alter i_e (Table 1). The second evoked method arises from the Poisson failure prediction which assumes low release probability (p) and derives m based on the total number of delivered stimuli (N_T) relative to the number failures (N_0), and is given by $m_f = ln(N_T/N_0)$. In control experiments, values of m derived from the failure method were ≈40% of those obtained empirically, possibly because p in these studies (unknown) is not optimally suited to fulfill the Poisson approximation. Nevertheless, results obtained using either method were consistent with those obtained by analyzing sEPSCs, revealing in both cases, that PACAP selectively increases quantal content (Fig. 6, Table 1). While quantal content

17

varied considerably across cultures such that overall values of m_e and m_f were only nominally larger for PACAP-treated neurons, PACAP did significantly increase quantal content within cultures. Thus m_e* and m_f* values were, respectively, 1.8- and 2.7-times higher for PACAP-treated neurons relative to control neurons evaluated in the same cultures ($p < 0.05$ for both; Table 1). Similarly, daily plots of m_e and m_f for PACAP treated *versus* control neurons reveal linear relationships having non-zero slopes for both that predicted 2.2- and 4.2-fold increases, respectively, in quantal content associated with PACAP treatment (Fig. 6C, D). The increases in quantal content occurred without detectable changes in mEPSC amplitudes (Table 1) indicating again that quantal size is unaffected by PACAP regulation. Based on these findings, it is concluded that PACAP rapidly enhances nicotinic transmission parameters (sEPSC F_s and I_s) by selectively altering presynaptic function, as indicated by its ability using three assays to increase mean quantal content independent of quantal size.

Nitric oxide production is required for PACAP-mediated synaptic effects. Increased quantal content was previously found to accompany long-term potentiation at nicotinic synapses on CG neurons *in situ*, and both were linked to elevated NO production (Lin and Bennett, 1994). Interestingly, PACAP stimulates production of neuronal nitric oxide synthase (nNOS), the enzyme critical for NO production (Bredt and Snyder, 1990) in pituitary gonadotrophs and dorsal root ganglion neurons and does so in a cAMP-, PKA-, and calmodulin-dependent manner (Bredt and Snyder, 1990; Bredt et al., 1992; Garrel et al., 2002). We therefore considered the hypothesis that PACAP/PAC$_1$R signaling enhances nicotinic synaptic function by activating NOS and subsequently increasing NO production (Fig. 7). The *first* test was to determine a NOS requirement by pre-treating cultures with the NOS inhibitor L-NAME and assessing subsequent PACAP-induced modulation of synaptic function. L-NAME (100 μM, 15 min) applied alone had no effect on basal synaptic transmission, but when PACAP was applied after L-NAME treatment, it failed to increase sEPSC F_s (Fig. 7A) or I_s (data not shown). Thus nNOS activity appears required for PACAP to enhance transmission at neuronal nicotinic synapses. The *second* test was to determine if exogenous NO mimics the actions and mechanism of PACAP induced synaptic modulation, and this also seems to be the case. Treating cultures with the NO donor, SNP (100 μM, 15 min), rapidly increased sEPSC F_s to levels that were indistinguishable from those produced by PACAP (Fig. 7A). Moreover, as with PACAP, the SNP-induced elevation of F_s was

18

accompanied by increased quantal content. The latter conclusion was reached because SNP treatment shifted the distribution of sEPSC amplitudes to significantly larger values (Fig. 7B) without changing the distribution of mEPSC amplitudes acquired from neurons in the same three cultures (Fig. 7C) thereby predicting an increase in m_s (= I_s/i_s). While these results do not identify obligatory signaling steps between PACAP/PAC$_1$, NOS/NO stimulation, and the relevant synaptic targets, they do indicate that PACAP/PAC$_1$ signaling alters nicotinic synaptic function by mechanisms that depend on NOS activation and subsequent release of NO.

DISCUSSION

The ability of PACAP to regulate nAChR function (Margiotta and Pardi, 1995; Pardi and Margiotta, 1999; Liu et al., 2000) and its localization to ACh-containing presynaptic terminals throughout the nervous system (Holgert et al., 1996; Braas et al., 1998; Calupca et al., 2000; Tornoe et al., 2000; Locknar et al., 2002; Richardson et al., 2003; Drescher et al., 2006) suggested that PACAP signaling would influence nAChR-mediated synaptic transmission. The present findings support this view, demonstrating that PACAP immunoreactivity disappears from cholinergic terminals on CG neurons following KCl depolarization and that PACAP activates PAC_1Rs and AC/PKA-dependent signaling to rapidly and persistently enhance nAChR-mediated synaptic transmission in CG cultures. Surprisingly, however, PACAP regulated synaptic function without influencing postsynaptic nAChRs (quantal size), but instead did so by increasing ACh release from presynaptic terminals (quantal content). Moreover, this presynaptic influence was dependent on NOS and subsequent mobilization of the gaseous messenger, NO. Taken together, the findings reveal that canonical PAC_1R- and NOS-dependent signaling mechanisms converge to regulate presynaptic function.

Levels of PACAP increase in the CG throughout embryonic development from E8 to E20 (Pugh and Margiotta, 2006), and cholinergic presynaptic terminal calyces that innervate ciliary neurons display intense PACAP immunoreactivity by E19 (Fig. 1 and Sumner et al., 2004). The subcellular distribution of PACAP within calyces is unknown, however, PACAP immunoreactivity has been localized to large dense core vesicles (80-120 nm diameter) typical for neuropeptides in presynaptic terminals providing input to hypothalamic paraventricular and spinal cord intermediolateral nucleus neurons (Chiba et al., 1996; Légrádi et al., 1997). Two major size classes of dense core vesicles, ($\approx$85 and $\approx$120 nm) have been identified in CG presynaptic terminals, with enkephalin and substance P both localizing to the smaller subclass (Erichsen et al., 1982), and from which enkephalin release has been demonstrated (Meriney et al., 1991). The specific vesicle class that contains PACAP and the impulse frequencies that best induce its release remain to be determined. In other autonomic preparations, however, depolarizing pulses delivered at $\approx$20 Hz release endogenous PACAP, and do so by a Ca^{2+}-dependent mechanism consistent with vesicular secretion (Katsoulis et al., 1996; Tornoe et al., 2000; Lamouche

20

and Yamaguchi, 2001; Tompkins et al., 2007). Since orthodromic transmission to ciliary neurons occurs reliably at stimulus frequencies of 25-100 Hz (Dryer and Chiappinelli, 1985; Chang and Berg, 1999) and sustained depolarization depletes PACAP from calyces (Fig. 1), it seems likely that these presynaptic terminals would release both ACh and PACAP at physiological firing frequencies.

PACAP application engages PAC_1Rs on CG neurons, activating canonical AC- and PKA-dependent signal cascades that rapidly and persistently increase the frequency and amplitude of sESPCs in culture (Figs. 2,3). We initially considered two plausible mechanisms to explain PACAP's actions on nicotinic synapses. The *first* was that PACAP might increase the excitability of CG neurons within the culture network, as it does for other autonomic neurons (Braas et al., 1998; DeHaven and Cuevas, 2004; Tompkins et al., 2007). This mechanism was excluded, however, because PACAP slightly raised action potential threshold and blocked repetitive firing (Fig. 4). While neither effect has been investigated further, the higher threshold is consistent with the sustained PACAP-induced depolarization increasing resting Na^+ channel inactivation (Hodgkin and Huxley, 1952). In addition, the blockade of repetitive firing may result from the ability of PACAP to elevate intracellular Ca^{2+} in CG neurons (Pardi and Margiotta, 1999; Woo and Margiotta, 2007), and thereby stimulate Ca^{2+}-activated small-conductance K^+ channels (Power and Sah, 2008) which are known to reduce repetitive firing (Pedarzani and Stocker, 2008; Louise Faber, 2009). Alternatively, PACAP might reduce transient A-type potassium (KA) channel currents which can support repetitive firing (Kim et al., 2005; Sonner and Stern, 2007) particularly at the modest firing frequencies seen here (Connor and Stevens, 1971). Consistent with this idea, PACAP reduced both KA channel currents and subunit expression in olfactory neurons (Han and Lucero, 2005, 2006).

The *second* possibility was that PACAP might increase α3*-nAChR mediated mEPSC amplitudes (i.e. quantal size). This seemed likely because we previously found that PACAP acting *via* PAC_1Rs, AC, and PKA rapidly increased whole cell-currents mediated by somatic α3*-nAChRs (Pardi and Margiotta, 1999) and because α3*-nAChRs underlie the vast majority of sEPSCs and mEPSCs detected here (Ullian et al., 1997; Chen et al., 2001). Surprisingly, however, PACAP failed to influence quantal size (Fig. 5, Table 1), and control experiments indicated this result did not arise from insufficient

21

resolution, the cell culture environment, or TTX treatment. Thus $\alpha3$*-nAChRs localized to the postsynaptic membrane, unlike those distributed elsewhere on the soma (Margiotta and Pardi, 1995; Pardi and Margiotta, 1999), appear refractory to regulatory influence by exogenous PACAP. Ultrastructural and autoradiographic studies, using toxin (*N*-Bgt) and antibody (mAb35) probes that recognize $\alpha3$*-nAChRs, do distinguish $\alpha3$*-nAChR populations on CG neurons based on their relative abundance and presence at postsynaptic *versus* extrasynaptic (i.e. non- and peri-synaptic) sites (Jacob et al., 1986; Loring and Zigmond, 1987; Shoop et al., 2001). In 5 d CG cultures, surface binding studies with these same reagents reveal $\approx10^5$ $\alpha3$*-nAChRs per neuron (Halvorsen and Berg, 1987), and by analyzing mAb35 and SV2 labeled confocal images, we estimate that 30% of mAb35 surface labeling is somatic and of this only 15% (corresponding to $\approx4,500$ $\alpha3$*-nAChRs) is localized in postsynaptic clusters (i.e. immediately adjacent to SV2 labeling; J.F. Margiotta and S.J. Jayakar, unpublished). Several features may distinguish low-abundance, postsynaptic $\alpha3$*-nAChRs from those distributed extrasynaptically. One is subunit stoichiometry since 80% of $\alpha3$*-nAChRs are assembled from $\alpha3$, $\alpha5$, and $\beta4$ nAChR subunits while 20% also contain $\beta2$ subunits (Vernallis et al., 1993; Conroy and Berg, 1995) raising the possibility that different proportions of the two $\alpha3$*-nAChR subtypes are present at post- *versus* extrasynaptic sites (see also(Sargent, 2009). A second distinguishing feature may be the degree to which post- and extra-synaptic $\alpha3$*-nAChRs associate with cytoplasmic scaffolding and/or anchoring proteins. $\alpha7$-nAChRs, for example, are linked to the F-actin scaffold, and disruption of this linkage dramatically alters their function (Liu and Berg, 1999). In addition, $\alpha3$*- and $\alpha7$-nAChRs on CG neurons associate with different PDZ proteins but it is not known if the $\alpha3$*-nAChR association with PSD-95 is obligatory or if it can also occur without (or with different) scaffolding proteins. In the CNS, association of synaptic NMDA receptors with PSD-95 provides a platform ensuring proximity to intracellular effectors and signaling cascades critical for synaptic function (Kennedy et al., 2005); the same may be true for nAChRs. We recently found that A-kinase anchoring proteins (AKAPs) are required for PACAP/PAC$_1$R PKA-dependent signaling to regulate synaptic function but not to enhance $\alpha3$*-nAChR currents (Jayakar et al., 2009). Lastly, endogenous PACAP present in CG calyces (Fig. 1) and in the cultures (Sumner and Margiotta, 2008) may act locally to potentiate postsynaptic $\alpha3$*-nAChRs such that exogenous PACAP has no further potentiating effect on

22

them. These considerations suggest that differences in subunit composition, association with scaffold and AKAP protein platforms, and prior history can influence the ways synaptic and extrasynaptic $\alpha3^*$-nAChRs respond to PACAP/PAC$_1$R-triggered intracellular signaling.

Since PACAP/PAC$_1$R signaling failed to influence quantal size, we sought to determine whether it enhanced presynaptic ACh release by increasing mean quantal content, m. Consistent with this idea was the initial observation that sEPSC amplitudes increased after PACAP treatment while mEPSC amplitudes remained unchanged, predicting a >50% increase in m_s (Table 1). Subsequent quantitative transmission studies, conducted by stimulating presynaptic axon fasicles to evoke EPSCs in target CG neuron somas, confirmed the involvement of a presynaptic mechanism (Fig. 6). In these studies, calculations based on the ratio of mean eEPSC to mEPSC amplitudes ($m_e = I_e/i_e$) and on transmission failures [$m_f = ln(N_T/N_0)$] predicted different quantal content values, possibly because the low p requirement of the Poisson model does not strictly apply. Nevertheless, PACAP significantly increased m using both methods of determination (Fig. 6, Table 1). It is unlikely that this conclusion results from misidentifying impulse failures as transmission failures. *First*, introducing impulse failures in a synaptic model reduced both m_e and m_f, and did so to similar degrees (J. Margiotta, unpublished). *Second*, since PACAP increases impulse threshold and lowers excitability (Fig. 4) it would be expected to increase impulse failures, biasing m_e and m_f to lower values. Such reductions in m are opposite to what is observed. The applicability of employing the EPSC amplitude ratio and Poisson failure methods in the evoked studies is supported by the observation that while m_e and m_f varied between experiments, they were linearly related in both control and PACAP-treated neuron pairs. Further, plotting m_e versus m_f obtained in different experiments resulted in slopes that were indistinguishable between control and PACAP-treated neurons (2.5 *versus* 1.8, respectively, p>0.05, data not shown). This latter finding indicates that PACAP alters quantal content without globally perturbing synaptic function. We hypothesize that the larger sEPSC amplitudes resulting from elevated quantal content would amplify the effects of PACAP throughout the culture network, bringing each interconnected neuron closer to impulse threshold and thereby causing even greater increases in F_s, as is observed.

In exploring how PACAP/PAC$_1$R signaling could enhance presynaptic transmitter release, we

uncovered an obligatory connection to NOS and subsequent release of the gaseous messenger, NO (Fig 7). Consistent with our findings, PACAP stimulates NOS and increases NO production in spinal cord nerve endings of dorsal root ganglion neurons (Mabuchi et al., 2004) by a mechanism likely involving NOS translocation to the plasma membrane (Ohnishi et al., 2008). In the CG system subcellular sites where PAC_1Rs might couple with NOS and thereby increase NO production are unknown. Since CG neuron cultures express both PAC_1Rs (this study and (Pugh and Margiotta, 2006) and NOS transcripts (Sumner and Margiotta, 2008), PAC_1Rs and NOS co-localized either in CG neuron somas or presynaptic terminals could, in principle, account for the effects observed here. Thus PAC_1R-mediated NOS activation would induce NO production at either site, allowing it to influence ACh release from presynaptic terminals by retrograde or direct mechanisms, respectively, as previously demonstrated in intracellular recordings from CG neurons conducted *in situ* (Scott and Bennett, 1993a; Scott and Bennett, 1993b; Lin and Bennett, 1994). In the ciliary ganglion, NOS is expressed in both neurons and presynaptic terminals (Nichol et al., 1995; Cuthbertson et al., 1999) and PAC_1Rs are abundant on freshly-dissociated CG neuron somas (Margiotta and Pardi, 1995; Pardi and Margiotta, 1999; Woo and Margiotta, 2007; Sumner and Margiotta, 2008). Since PAC_1R transcripts are absent from neurons providing presynaptic input to the CG (Peeters et al., 2000) and Peeters, personal communication), however, the locus of NOS and PAC_1R interaction *in situ* may be confined to CG neuron somas. Consistent with this constraint and with a requirement for AC/PKA-dependent processes to enhance synaptic function (Fig. 3), PAC_1R transduction *via* AC and PKA increases CG neuron somatic cAMP and, by the resulting enhanced $\alpha3^{*}$- and $\alpha7$-nAChR-mediated currents (Margiotta and Pardi, 1995; Pardi and Margiotta, 1999), elevates somatic Ca^{2+} (Verino et al., 1992; Bertrand et al., 1993; Séguéla et al., 1993). Both cAMP and Ca^{2+} are known to stimulate NOS (Oess et al., 2006; Ohnishi et al., 2008) an action that would increase somatic NO output and thus be expected to influence presynaptic ACh release in a retrograde fashion. Interestingly, a retrograde signal regulates ACh release at nicotinic synapses in mouse sympathetic ganglia where a disruption in the $\alpha3$-nAChR subunit gene abolishes synaptic transmission and $\alpha3$-nAChR mediated currents (Rassadi et al., 2005). In that case, the loss of postsynaptic activity impairs presynaptic ACh release by reducing high-affinity choline transporter (CHT) function and expression (Krishnaswamy and Cooper,

2009). Increased CHT expression could similarly underlie the enhanced synaptic function induced by PACAP in CG neuron cultures that persists for days after exposures of only minutes. Indeed, in a recent gene array study, brief PACAP exposure (15 min, followed by 6h incubation in normal culture medium) upregulated CHT transcripts to levels that were 2.1 times those of sham-treated controls (Sumner and Margiotta, 2008). Interestingly, gene transcripts encoding choline acetyltransferase and synaptotagmin IV were similarly increased after brief PACAP exposure (Sumner and Margiotta, 2008). Thus PACAP rapidly upregulates the expression of transcripts encoding presynaptic proteins involved not only in choline transport, but also in ACh synthesis and release, all of which could sustain enhanced synaptic function consistent with the core findings reported here.

The actions of PACAP/PAC$_1$R signaling on synapses are similar to nicotinic long-term potentiation (LTP) previously described in the intact CG (Scott and Bennett, 1993b) because both have a presynaptic locus and share NOS/NO dependence (Figs. 5-7). As mentioned above, PACAP is released by delivering presynaptic stimuli at ≈20 Hz in other autonomic preparations (Tornoe et al., 2000; Lamouche and Yamaguchi, 2001; Tompkins et al., 2007). Since these frequencies are similar to the 30 Hz necessary to induce LTP in the CG (Scott and Bennett, 1993b) and are expected to release both ACh and PACAP, the subsequent PAC$_1$R-generated signaling demonstrated here may be required for LTP. The long-lasting effects of even brief PACAP exposure (Fig. 2 and (Sumner and Margiotta, 2008) further suggest that its release need not be sustained for the peptide to exert long term effects on neurotransmission and other critical processes. Thus PACAP's broad expression, colocalization with ACh, and its rapid-onset yet persistent effects on nAChR-mediated transmission seen here, suggest PACAP will emerge as a critical modulator of nicotinic synapses throughout the nervous system.

REFERENCES

Bekkers JM, Stevens CF (1995) Quantal analysis of EPSCs recorded from small numbers of synapses in hippocampal cultures. J Neurophysiol 73:1145-1156.

Bertrand D, Galzi J, Devillers-Thiéry A, Bertrand S, Changeux J-P (1993) Mutations at two distinct sites within the channel domain M2 alter calcium permeability of neuronal $\alpha 7$ nicotinic receptor. Proc Natl Acad Sci U S A 90:6971-6975.

Braas K, May V, Harakall S, Hardwick J, Parsons R (1998) Pituitary adenylate cyclase-activating polypeptide expression and modulation of neuronal excitability in guinea pig cardiac ganglia. J Neurosci 18:9766-9779.

Braas KM, Schutz KC, Bond JP, Vizzard MA, Girard BM, May V (2007) Microarray analyses of pituitary adenylate cyclase activating polypeptide (PACAP)-regulated gene targets in sympathetic neurons. Peptides 28:1856-1870.

Bredt DS, Snyder SH (1990) Isolation of nitric oxide synthetase, a calmodulin-requiring enzyme. Proc Natl Acad Sci USA 87:682-685.

Bredt DS, Ferris CD, Snyder SH (1992) Nitric oxide synthase regulatory sites. Phosphorylation by cyclic AMP-dependent protein kinase, protein kinase C, and calcium/calmodulin protein kinase; identification of flavin and calmodulin binding sites. J Biol Chem 267:10976-10981.

Calupca MA, Vizzard MA, Parsons R (2000) Origin of pituitary adenylate cyclase-activating polypeptide (PACAP)-immunoreactive fibers innervating guinea pig parasympathetic cardiac ganglia. J Comp Neurol 423:26-39.

Cantino D, Mugnaini E (1975) The structural basis for electrotonic coupling in the avian ciliary ganglion. J Neurocytol 4:505-536.

Chang K, Berg D (1999) Nicotinic acetylcholine receptors containing $\alpha 7$ subunits are required for reliable synaptic transmission *in situ*. J Neurosci 19:3701-3710.

Chen M, Pugh P, Margiotta J (2001) Nicotinic synapses formed between chick ciliary ganglion neurons

in culture resemble those present on the neurons *in vivo*. J Neurobiol 47:265-279.

Chiba T, Tanaka K, Tatsuoka H, Dun SL, Dun NJ (1996) The synaptic structure of PACAP immunoreactive axons in the intermediolateral nucleus of the rat. Neurosci Lett 214:65-68.

Connor JA, Stevens CF (1971) Prediction of repetitive firing behaviour from voltage clamp data on an isolated neurone soma. The Journal of Physiology 213:31-53.

Conroy WG, Berg DK (1995) Neurons can maintain multiple classes of nicotinic acetylcholine receptors distinguished by different subunit compositions. J Biol Chem 270:4424-4431.

Conroy WG, Nai Q, Ross B, Naughton G, Berg DK (2007) Postsynaptic neuroligin enhances presynaptic inputs at neuronal nicotinic synapses. Dev Biol 307:79-91.

Csernus V, Schally A, Groot K (1999) Effect of GHRH and peptides from the vasoactive intestinal peptide family on cAMP production of human cancer cell lines *in vitro*. Journal of Endocrinology 163:269-280.

Cuthbertson S, Zagvazdin YS, Kimble TD, Lamoreaux WJ, Jackson BS, Fitzgerald ME, Reiner A (1999) Preganglionic endings from nucleus of Edinger-Westphal in pigeon ciliary ganglion contain neuronal nitric oxide synthase. Vis Neurosci 16:819-834.

DeHaven W, Cuevas J (2004) VPAC receptor modulation of neuroexcitability in intracardiac neurons. Journal of Biological Chemistry 279:40609-40621.

del Castillo J, Katz B (1954) Quantal components of the end-plate potential. J Physiol 124:560-573.

Drescher MJ, Drescher DG, Khan KM, Hatfieldd JS, Ramakrishnana NA, Abu-Hamdana MD, Lemonniera LA (2006) Pituitary adenylyl cyclase-activating polypeptide (PACAP) and its receptor (PAC1-R) are positioned to modulate afferent signaling in the cochlea. Neuroscience 142:139-164.

Dryer SE, Chiappinelli VA (1985) Properties of choroid and ciliary neurons in the avian ciliary ganglion and evidence for substance P as a neurotransmitter. J Neurosci 5:2654-2661.

Erichsen JT, Karten HJ, Eldred WD, Brecha NC (1982) Localization of substance P-like and

enekphalin-like immunoreactivity within preganglionic terminals of the avain ciliary ganglion: light and electron microscopy. J Neurosci 2:994-1003.

Ermilov L, Schmalz P, Miller S, Szurszewski J (2004) PACAP modulation of the colon-inferior mesenteric ganglion reflex in the guinea pig. J Physiol 560.1:231-247.

Gadea A, López E, López-Colomé A (1999) The adenylate cyclase inhibitor MDL-12330A has a non-specific effect on glycine transport in Müller cells from the retina. Brain Research 838:200-204.

Garrel G, Lozach A, Bachir L, Laverriere J-N, Counis R (2002) Pituitary adenylate cyclase-activating polypeptide stimulates nitric oxide synthase type I expression and potentiates the cGMP response to gonadotropin-releasing hormone of rat pituitary gonadotrophs. J Biol Chem 277:46391-46401.

Girard B, Keller E, Schutz K, May V, Braas K (2004) Pituitary adenylate cyclase activating polypeptide and PAC1 receptor signaling increase Homer 1a expression in central and peripheral neurons. Regulatory Peptides 123:107-116.

Glass D, Cheng H, Mende-Mueller L, Reed J, Walsh D (1989) Primary structural determinants essential for potent inhibition of cAMP-dependent protein kinase by inhibitory peptides corresponding to the active portion of the heat-stable inhibitor protein. J Biol Chem 264:8802-8810.

Guellan G, Mahu J, Mavier P, Berthelot P, Hanoune J (1977) RMI 12330 A, an inhibitor of adenylate cyclase in rat liver. Biochimica and Biophysica Acta 484:465-475.

Halvorsen SW, Berg DK (1987) Affinity labeling of neuronal acetylcholine receptor subunits with an α-neurotoxin that blocks receptor function. J Neurosci 7:2547-2555.

Hamelink C, Tjurmina O, Damadzic R, Young W, Weihe E, Lee H-W, Eiden L (2002) Pituitary adenylate cyclase-activating polypeptide is a sympathoadrenal neurotransmitter involved in catecholamine regulation and glucohomeostasis. Proc Natl Acad Sci USA 99:461-466.

Han P, Lucero MT (2005) Pituitary adenylate cyclase activating polypeptide reduces A-type K+ currents and caspase activity in cultured adult mouse olfactory neurons. Neuroscience 134:745-756.

Han P, Lucero MT (2006) Pituitary adenylate cyclase activating polypeptide reduces expression of

28

Kv1.4 and Kv4.2 subunits underlying A-type K(+) current in adult mouse olfactory neuroepithelia. Neuroscience 138:411-419.

Hannibal J (2002) Pituitary adenylate cyclase-activating peptide in the rat central nervous system: an immunohistochemical and in situ hybridization study. J Comp Neurol 453:389-417.

Hess A (1965) Developmental changes in the structure of the synapse on the myelinated cell bodies of the chicken ciliary ganglion. J Cell Biol 25:1-19.

Hodgkin A, Huxley A (1952) The dual effect of membrane potential on sodium conductance in the giant axon of Loligo. The Journal of Physiology 116:497-506.

Holgert H, Holmberg K, Hannibal J, Fahrenkrug J, Brimijoin S, Hartman BK, Hokfelt T (1996) PACAP in the adrenal gland - relationship with choline acetyltransferase, enkephalin and chromaffin cells and effects of immunological sympathectomy. NeuroReport 8:297-301.

Jacob M, Lindstrom J, Berg D (1986) Surface and intracellular distribution of a putative neuronal nicotinic acetylcholine receptor. J Cell Biol 103:205-211.

Jayakar S, Pugh P, Margiotta J (2009) A-kinase anchoring proteins participate in regulating transmission at neuronal nicotinic synapses. Neuroscience Meeting Planner, Chicago, IL: Society for Neuroscience, 2009 Online.

Johnston D, Wu SM-S (1995) Foundations of cellular neurophysiology. Cambridge: The MIT Press.

Kanda N, Watanabe S (2001) Intracellular 3',5'-adenosine cyclic monophosphate level regulates house dust mite-induced interleukin-13 production by T cells from mite-sensitive patients with atopic dermatitis. Journal of Investigative Dermatology 116:3-11.

Katsoulis S, Schmidt W, Schwarzhoff R, Fossch U, Jin J-G, Grider J, Makhlouf G (1996) Inhibitory transmission in guinea pig stomach mediated by distinct receptors for pituitary adenylate cyclase-activating peptide. Journal of Pharmacology and Experimental Theraupeutics 278:199-204.

Kennedy M, Beale H, Carlisle H, Washburn L (2005) Integration of biochemical signalling in spines. Nat Rev Neurosci 6:423-434.

Kim J, Wei DS, Hoffman DA (2005) Kv4 potassium channel subunits control action potential repolarization and frequency-dependent broadening in rat hippocampal CA1 pyramidal neurones. The Journal of Physiology 569:41-57.

Kimura H (2000) Hydrogen sulfide induces cyclic AMP and modulates the NMDA receptor. Biochemical and Biophysical Research Communications 267:129-133.

Krishnaswamy A, Cooper E (2009) An activity-dependent retrograde signal induces the expression of the high-affinity choline transporter in cholinergic neurons. Neuron 61:272-286.

Lamouche S, Yamaguchi N (2001) Role of PAC1 receptor in adrenal catecholamine secretion induced by PACAP and VIP in vivo. Am J Physiol Regul Integr Comp Physiol 280:R510-R518.

Landmesser L, Pilar G (1972) The onset and development of transmission in the chick ciliary ganglion. J Physiol 222:691-713.

Légrádi G, Hannibal J, Lechan RM (1997) Association between pituitary adenylate cyclase-activating polypeptide and thyrotropin-releasing hormone in the rat hypothalamus. J Chem Neuroanat 13:265-279.

Lin Y, Bennett M (1994) Nitric oxide modulation of quantal secretion in chick ciliary ganglia. Journal of Physiology 481.2:385-394.

Liu D-M, Cuevas J, Adams DJ (2000) VIP and PACAP potentiation of nicotinic ACh-evoked currents in rat parasympathetic neurons is mediated by G-protein activation. Eur J Physiol 12:2243-2251.

Liu QS, Berg DK (1999) Actin filaments and the opposing actions of CaM Kinase II and calcineurin in regulating alpha7-containing nicotinic receptors on chick ciliary ganglion neurons. J Neurosci 19:10280-10288.

Locknar SA, Calupca MA, Parsons RL (2002) Innervation of guinea-pig stellate ganglia by nitric oxide synthase, cocaine- and amphetamine-regulated transcript protein- and pituitary adenylate cyclase activating polypeptide-immunoreactive fibers. Neuroscience 112:525-533.

Loring R, Zigmond R (1987) Ultrastructural distribution of 125I-Toxin F binding sites on chick ciliary neurons: synaptic localization of a toxin that blocks ganglionic nicotinic receptors. Journal of

Neuroscience 7:2153-2162.

Louise Faber ES (2009) Functions and Modulation of Neuronal SK Channels. Cell Biochem Biophys.

Mabuchi T, Shintani N, Matsumura S, Okuda-Ashitaka E, Hashimoto H, Muratani T, Minami T, Baba A, Ito S (2004) Pituitary adenylate cyclase-activating polypeptide is required for the development of spinal sensitization and induction of neuropathic pain. J Neurosci 24:7283-7291.

Margiotta J, Pardi D (1995) Pituitary adenylate cyclase-activating polypeptide type I receptors mediate cyclic AMP-dependent enhancement of neuronal acetylcholine sensitivity. Mol Pharmacol 48:63-71.

Margiotta J, Berg D, Dionne V (1987) Cyclic AMP regulates the proportion of functional acetylcholine receptors on chick ciliary ganglion neurons. Proc Natl Acad Sci U S A 84:8155-8159.

Margiotta JF, Berg DK (1982) Functional synapses are established between ciliary ganglion neurons in dissociated cell culture. Nature 296:152-154.

Martin AR, Pilar G (1964) Quantal components of the synaptic potential in the ciliary ganglion of the chick. J Physiol 175:1-16.

McIntosh J, Santos A, Olivera B (1999) *Conus* peptides targeted to specific nicotinic acetylcholine receptor subtypes. Annu Rev Biochem 68.

Meriney SD, Ford MJ, Oliva D, Pilar G (1991) Endogenous opioids modulate neuronal survival in the developing avian ciliary ganglion. J Neurosci 11:3705-3717.

Miyata A, Arimura A, Dahl R, Minamino N, Uehara A, Jiang L, Culler M, Coy D (1989) Isolation of a novel 38 residue-hypothalamic polypeptide which stimulates adenylate cyclase in pituitary cells. Biochem Biophys Res Commun 164:567-574.

Mohamed AS, Rivas-Plata KA, Kraas JR, Saleh SM, Swope SL (2001) Src-Class Kinases Act within the Agrin/MuSK Pathway to Regulate Acetylcholine Receptor Phosphorylation, Cytoskeletal Anchoring, and Clustering. J Neurosci 21:3806-3818.

Moro O, Lerner E (1997) Maxadilan, the vasodilator from sand flies, is a specific pituitary adenylate

cyclase activating peptide type I receptor agonist. Journal of Biological Chemistry 272:966-970.

Moro O, Wakita K, Ohnuma M, Denda S, Lerner E, Tajima M (1999) Functional characterization of structural alterations in the sequence of the vasodilatory peptide maxadilan yields a pituitary adenylate cylcase-activating peptide type 1 receptor-specific antagonist. Journal of Biological Chemistry 274:23103-23110.

Nai Q, Mcintosh JM, Margiotta JF (2003) Relating neuronal nicotinic acetylcholine receptor subtypes defined by subunit composition and channel function. Molecular Pharmacology 63:311-324.

Nichol K, Chan N, Davey D, Bennett M (1995) Location of nitric oxide synthase in the developing avian ciliary ganglion. Journal of the Autonomic Nervous System 51:91-102.

Oess S, Icking A, Fulton D, Govers R, Müller-Esterl W (2006) Subcellular targeting and trafficking of nitric oxide synthases. Biochem J 396:401-409.

Ohnishi T, Okuda-Ashitaka E, Matsumura S, Katano T, Nishizawa M, Ito S (2008) Characterization of signaling pathway for the translocation of neuronal nitric oxide synthase to the plasma membrane by PACAP. J Neurochem 105:2271-2285.

Pardi D, Margiotta JF (1999) Pituitary adenylate cyclase-activating polypeptide activates a phospholipase C-dependent signal pathway in chick ciliary ganglion neurons that selectively inhibits α7-containing nicotinic receptors. J Neurosci 19:6327-6337.

Paysan J, Conroy W, Coggan J, Berg D (2000) The neurofilament infrastructure of a developing presynaptic calyx. J Comp Neurol 425:284-294.

Pedarzani P, Stocker M (2008) Molecular and cellular basis of small--and intermediate-conductance, calcium-activated potassium channel function in the brain. Cell Mol Life Sci 65:3196-3217.

Peeters K, Gerets HHJ, Arckens L, Vandesande F (2000) Distribution of pituitary adenylate cyclase-activating polypeptide and pituitary adenylate cyclase-activating polypeptide type I receptor mRNA in the chicken brain. J Comp Neurol 423:66-82.

Power J, Sah P (2008) Competition between Calcium-Activated K+ Channels Determines Cholinergic Action on Firing Properties of Basolateral Amygdala Projection Neurons. Journal of

32

Neuroscience 28:3209-3220.

Pugh P, Margiotta J (2000) Nicotinic acetylcholine receptor agonists promote survival and reduce apoptosis of chick ciliary ganglion neurons. Mol Cell Neurosci 15:113-122.

Pugh P, Margiotta J (2006) PACAP support of neuronal survival requires MAPK- and activity-generated signals. Molecular and Cellular Neuroscience 31:586-595.

Rasband W (2004) ImageJ. In, 1.33u Edition: National Institutes of Health, Bethesda, Maryland USA.

Rassadi S, Krishnaswamy A, Pié B, McConnell R, Jacob MH, Cooper E (2005) A null mutation for the alpha3 nicotinic acetylcholine (ACh) receptor gene abolishes fast synaptic activity in sympathetic ganglia and reveals that ACh output from developing preganglionic terminals is regulated in an activity-dependent retrograde manner. J Neurosci 25:8555-8566.

Rathouz MM, Vijayaraghavan S, Berg DK (1995) Acetylcholine differentially affects intracellular calcium via nicotinic and muscarinic receptors on the same population of neurons. J Biol Chem 270:14366-14375.

Ravdin PM, Berg DK (1979) Inhibition of neuronal acetylcholine sensitivity by α-toxins from *Bungarus multicinctus* venom. Proc Natl Acad Sci USA 76:2072-2076.

Rawlings SR (1994) At the cutting edge: PACAP, PACAP receptors and intracellular signaling. Mol Cell Endocrinol 101:C5-C9.

Richardson RJ, Grkovic I, Anderson CR (2003) Immunohistochemical analysis of intracardiac ganglia of the rat heart. Cell Tissue Res 314:337-350.

Role LW, Fischbach GD (1987) Changes in the number of chick ciliary ganglion neuron processes with time in cell culture. Journal of Cell Biology 104:363-370.

Rubio M, Curcio C, Chauvet N, Bruses J (2005) Assembly of the N-cadherin complex during synapse formation involves uncoupling of p120-catenin and association with presenilin 1. Mol Cell Neurosci 30:611-623.

Sargent PB (2009) Nicotinic receptors concentrated in the subsynaptic membrane do not contribute

significantly to synaptic currents at an embryonic synapse in the chicken ciliary ganglion. J Neurosci 29:3749-3759.

Scott T, Bennett M (1993a) The effect of nitric oxide on the efficacy of synaptic transmission through the chick ciliary ganglion. Br J Pharmacol 110:627-632.

Scott TRD, Bennett MR (1993b) The effect of ions and second messengers on long-term potentiation of chemical transmission in avian ciliary ganglia. Br J Pharmacol 110:461-469.

Séguéla P, Wadiche J, Dineley-Miller K, Dani J, Patrick J (1993) Molecular cloning, functional properties, and distribution of rat brain α7: a nicotinic cation channel highly permeable to calcium. J Neurosci 13:596-604.

Shoop RD, Chang KT, Ellisman MH, Berg DK (2001) Synaptically driven calcium transients via nicotinic receptors on somatic spines. J Neurosci 21:771-781.

Sonner PM, Stern JE (2007) Functional role of A-type potassium currents in rat presympathetic PVN neurones. J Physiol (Lond) 582:1219-1238.

Sumner A, Margiotta JF (2008) Pituitary adenylate cyclase-activating polypeptide (PACAP) alters parasympathetic neuron gene expression in a time-dependent fashion. J Mol Neurosci 36:141-156.

Sumner A, Przepyszny L, Margiotta J (2004) PACAP localizes to presynaptic terminals and activates CREB in ciliary ganglion neurons. Society for Neuroscience Abstract Viewer 2004:847.814.

Tompkins J, Ardell J, Hoover D, Parsons R (2007) Neurally released pituitary adenylate cyclase-activating polypeptide enhances guinea pig intrinsic cardiac neurone excitability. The Journal of Physiology 582:87-93.

Tornoe K, Hannibal J, Jensen TB, Georg B, Rickelt LF, Andreasen MB, Fahrenkrug J, Holst JJ (2000) PACAP-(1-38) as neurotransmitter in the porcine adrenal glands. Am J Physiol Endocrinol Metab 279:E1413-E1425.

Ullian EM, McIntosh JM, Sargent PB (1997) Rapid synaptic transmission in the avian ciliary ganglion is mediated by two distinct classes of nicotinic receptors. J Neurosci 17:7210-7219.

34

Vaudry D, Gonzalez B, Basille M, Yon L, Fournier A, Vaudry H (2000) Pituitary adenylate cyclase-activating polypeptide and its receptors: from structure to functions. Pharmacological Reviews 52:269-324.

Verino S, Amador M, Luetje CW, Patrick J, Dani JA (1992) Calcium modulation and high calcium permeability of neuronal nicotinic acetylcholine receptors. Neuron 8:127-134.

Vernallis AB, Conroy WG, Berg DK (1993) Neurons assemble AChRs with as many as 3 kinds of subunits while maintaining subunit segregation among subtypes. Neuron 10:451-464.

Wang K, Hackett JT, Cox ME, Van Hoek M, Lindstrom JM, Parsons SJ (2004) Regulation of the neuronal nicotinic acetylcholine receptor by SRC family tyrosine kinases. J Biol Chem 279:8779-8786.

Wilson Horch H, Sargent P (1995) Perisynaptic surface distribution of multiple classes of nicotinic acetylcholine receptors on neurons in the chicken ciliary ganglion. J Neurosci 15:7778-7795.

Woo S, Margiotta J (2007) PACAP elevates calcium in ciliary ganglion neurons by PAC1-mediated signaling. In: 8th International Symposium for VIP, PACAP and Related Peptides. Manchester, VT.

Zhou X, Nai Q, Chen M, Dittus JD, Howard MJ, Margiotta JF (2004) Brain-derived neurotrophic factor and trkB signaling in parasympathetic neurons: relevance to regulating α7-containing nicotinic receptors and synaptic function. Journal of Neuroscience 24:4340-4350.

Article I.   FIGURE LEGENDS

Figure 1.   PACAP localizes to presynaptic terminals and is released by depolarization. **Left**: Synapsin I (**A**, green) and PACAP (**B**, red) immunostaining co-localize (**C**, yellow) in presynaptic calyces that contact ciliary ganglion neurons. **Right:** After incubation with depolarizing levels of KCl (50 mM, 30 min), Synapsin I immunostaining remains (**D**) while PACAP immunostaining disappears from the calyces (**E, F**). Confocal images were acquired from E19 ciliary ganglia and depict representative, 1 μm optical sections. Scale bar, 20 μm.

Figure 2.   PACAP enhances transmission at nicotinic synapses on CG neurons.   **A.** Representative sEPSCs are depicted for sham- and PACAP-treated (100 nM, 15 min) CG neurons from the same culture. In this experiment, PACAP increased mean sEPSC frequency (F_s) from 1.5 to 7.7 Hz, and mean sEPSC amplitude (I_s) from 22.1 to 31.5 pA (n = 5 neurons for both). Calibrations, 10 pA/100 ms. **B** and **C.** Cumulative distributions of F_s (**B**) and I_s (**C**) values obtained from PACAP-treated neurons (■,●; n = 146) are plotted with accompanying values from sham-treated control neurons (□, ○; n = 154) tested in the same 30 experiments. Significant rightward shifts in both F_s and I_s distributions are associated with PACAP treatment (p < 0.02, by Kolmogorov-Smirnov test). The bar graph insets show that the PACAP treated neurons displayed mean sEPSC frequency and amplitude values that were, 3.8 ± 0.3 and 1.4 ± 0.1 times larger (F_s* and I_s*, respectively) than those of sham-treated controls (*p* < 0.05 for both, *t*-test). **D** and **E.** Brief PACAP exposure produces persistent increases in sEPSC frequency and amplitude. Washout kinetics were assessed by comparing F_s* (**D**) and I_s* (**E**) at the indicated times after 15 min PACAP (100 nM) treatment (■, ●) relative to sham treatments (□, ○). CG neurons were treated with PACAP for 15 minutes on the 3rd (48 h wash), 4th (24 h wash), or 5th (<30 min wash) day in culture, or not at all. Both F_s* and I_s* remain elevated in PACAP-compared to sham-treated control neurons for at least 48h. In this and subsequent figures, value asterisks (*) indicate a significant change (*p* < 0.05) relative to controls.

Figure 3.   PACAP regulates synaptic function *via* PAC_1R activation of AC-dependent signaling. **A.** PACAP (1-100 nM, 15 min, 37°C) produced dose-dependent increases in sEPSC frequency (F_s*, ■, black line, left axis) and amplitude (I_s*, ●, blue line, right axis) predicting nanomolar EC_{50} values for both

36

(6.4 ± 2.2 nM and 6.9 ± 2.5 nM, respectively) while VIP (100 nM) failed to increase either F_s* (𝔸) or I_s* (𝔸). Both findings are consistent with a requirement for PAC_1R over VPACR activation. **B.** PLC is dispensable for PACAP-mediated changes. Activation of PLC signaling with muscarine (100 µM) failed to alter F_s*. Similarly, PLC inhibition with U73122 (1 µM, U7) failed to change F_s* or to prevent PACAP from enhancing F_s*. Similar effects on sEPSC amplitudes (I_s*) were observed (data not shown). **C.** Cyclic AMP, AC and PKA are required for sustained PACAP modulation of sEPSCs. 8Br-cAMP (2 mM) mimicked PACAP's actions while AC inhibition with MDL12330A (+MDL, 1 µM) or PKA with myristolated PKI (+PKI, 1 µM) reduced the ability of PACAP (100 nM, 15 min) to enhance sEPSC frequency (F_s*). Similar effects on sEPSC amplitudes (I_s*) were observed, and neither MDL12330A nor myristolated PKI altered sEPSC frequency or amplitude when applied alone (data not shown).

Figure 4. PACAP reduces the excitability of CG neurons. **A.** Example records depict increased action potential firing associated with application of progressively larger depolarizing currents in sham-treated control neurons (left) while firing was depressed after PACAP treatment (100 nM, 15 min, right). Traces show voltage recordings from neurons in whole-cell current clamp mode with 200 ms duration current pulses (bars above records) applied as indicated (I_{inj}) at 0.1 Hz. **B.** The number of action potentials increased as a function of the applied depolarizing current intensity in sham-treated control neurons (◇, n = 8) but not in PACAP-treated neurons (◆, n = 8). Linear regression analyses predicted slopes of 0.039 pA^{-1} for control and and 0.001 pA^{-1} for PACAP-treated neurons ($p < 0.0001$, F test).

Figure 5. PACAP fails to influence α3*-nAChR mediated mEPSC amplitudes (i_s) while enhancing somatic membrane α3*-nAChR responses. **A.** Example records showing spontaneous mEPSCs (▲) with similar amplitudes in control (top) and PACAP-treated (bottom, 100 nM, 15 min) CG neurons from the same experiment. Scale bars, 10 pA/10 msec. **B.** Stability of mean mEPSC amplitudes in control (○, n = 19, 807 events) and PACAP-treated neurons (●, n = 26, 1273 events) from four experiments. Solid line indicates the mean mEPSC amplitude (7.2 pA) ± 1 SD (1.8 pA; dashed lines) from 37 neurons in 9 experiments. **C and D** show detailed comparisons of mean mEPSC frequencies (**C**) and amplitudes (**D**) from PACAP-treated (●, ■) and control (○, □) CG neurons acquired in the same 4 experiments as in **B**. Cumulative distributions reveal that PACAP treatments shift mEPSC frequencies

37

(f_s, left) to slightly higher maximal values ($p < 0.05$, KS test) without detectably changing mEPSC amplitudes (i_s, right, $p > 0.6$, KS test). Bar plots show that mean (± SEM) f_s (left) and i_s (right) values after PACAP treatment (n = 23; 0.57 ± 0.09 Hz and 7.9 ± 0.3 pA, respectively) were indistinguishable from those obtained from matched controls (n = 18; 0.39 ± 0.04 Hz and 7.1 ± 0.3 pA, respectively) tested in parallel ($p > 0.09$ for both, t-test). Results in **A - D** were obtained in the presence of 1 µM TTX. **E.** PACAP treatment increases inward currents generated by plasma membrane α3*-nAChRs. In these experiments, α3*-nAChRs were isolated by pre-incubating cultures in αBgt (50 nM, 1 h) (Nai et al., 2003; Zhou et al., 2004) with toxin exposure continued throughout the indicated treatments. Records (left) depict membrane α3*-nAChR currents acquired from sham- and PACAP-treated neurons (black and gray traces, respectively) that were induced by 20 µM nicotine delivered by rapid pressure microperfusion (1 sec @ 7.5 psi; top bar). Scale bars: 200 pA/250 msec. Bar graph (right) shows that peak α3*-nAChR responses (pA/pF) induced by nicotine in PACAP-treated neurons (black bar) were 2.4 ± 0.1 times larger than those obtained from sham-treated control neurons from the same experiments (n = 4 for each). Following TTX (1 µM) pre-incubation and inclusion in the recording solution, PACAP treatment (check bar) similarly increased nicotine induced peak α3*-nAChR responses to 2.5 ± 0.4 times control values (n = 4 for each). TTX treatment alone had no detectable effect. Asterisks indicate a significant difference in α3*-nAChR response relative to controls ($p < 0.01$, ANOVA).

Figure 6. Evoked EPSCs and quantal analysis in CG neuron cultures. **A.** Stimulating neurite fasicles (Stim, 1-4) converging onto a CG neuron soma "hub" (center, recording pipette at right, Rec) reliably evokes somatic EPSCs (1-3), which are absent when a non-convergent fasicle is stimulated (4). **B.** Sample recordings show that single fasicle stimuli (▼) either evoke (+) or fail to evoke (-) a short-latency EPSC in the associated "hub" soma. Spontaneous sEPSCs (solid) and mEPSCs (dashed) are circled. Calibrations: 20 pA/10 ms. **C-D.** Quantal content was assessed for individual control and PACAP-treated neurons using $m_e = I_e/i_e$ or $m_f = ln(N_T/N_0)$. In **C** and **D**, respectively, each point represents the average m_e or m_f value (± SEM, n = 2 to 8 neurons for each treatment per day) from 3 experiments. Linear regression lines drawn through the points ($r^2 \approx 0.8$) both had non-zero positive slopes (p < 0.001 by F-test, slope = $\Delta m = \Delta m_{PACAP} / \Delta m_{Control}$) indicating that PACAP treatment increased

38

m_e and m_f by 2.2 ± 0.5- and 4.2 ± 0.7-fold, respectively.   Quantal content comparisons within experiments yielded a similar trend predicting m_e and m_f values for PACAP treated neurons that were, respectively, 1.8 ± 0.3- and 2.7 ± 0.7-times higher than those obtained from sham treated control neurons tested in parallel (Table 1).

Figure 7.   PACAP enhances synaptic activity *via* NOS activation and NO production. **A.** Effects of NOS inhibition and NO production.   The stimulation of sEPSC frequency (F_s*) normally seen for PACAP-treated neurons (black bar) relative to sham controls tested in parallel (white bar, n = 5 for each) was blocked after inhibiting NOS with L-NAME (100 μM, checked bar, n = 4) while L-NAME alone had no discernable effect (gray bar, n = 4). Mimicking NOS activation with the NO donor SNP (100 μM, green bar, n = 8) increased F_s to a level significantly above untreated controls (n = 8) and indistinguishable from that achieved after PACAP treatment. Asterisks (*) indicate *p* < 0.05 *versus* Control; § indicates *p* < 0.05 *versus* PACAP treatment alone. F_s* values obtained after L-NAME treatment were indistinguishable from those obtained after control or PACAP/L-NAME treatments (p > 0.05 for both). **B, C.** Like PACAP, NO production increases quantal content inferred from sEPSCs. SNP treatment (green filled boxes) significantly increased I_s relative to untreated controls (open boxes; n = 8 for each), but left i_s unchanged relative to controls (n = 9 for each). The distribution of sEPSC amplitudes (I_s, **B**) exhibited a significant rightward shift after SNP treatment compared to controls (2113 and 1375 events from 8 PACAP-treated and 8 control neurons, respectively, *p* < 0.01, KS test), while mEPSC amplitudes (i_s, **C**) remained unaltered (437 and 467 events from 9 PACAP-treated and 9 control neurons, respectively, *p* = 0.078, KS test) thereby predicting increased m_s (= I_s/i_s).

Table 1. Actions of PACAP on transmission parameters at neuronal nicotinic synapses.

	Spontaneous EPSCs		Evoked EPSCs		EPSC Failures	
	Control	PACAP	Control	PACAP	Control	PACAP
Quantal Size, i (pA)	7.1 ± 0.3 (18)	7.9 ± 0.3 (23)	8.1 ± 0.2 (15)	8.4 ± 0.5 (10)	--	--
i^*	1.11 ± 0.04		1.05 ± 0.07		--	
Quantal Content, m	2.0 ± 0.3 (19)	[#]2.9 ± 0.3 (16)	1.7 ± 0.3 (15)	2.9 ± 0.6 (10)	0.5 ± 0.1 (15)	1.0 ± 0.5 (10)
m^*	[#]1.57 ± 0.18		[#]1.81 ± 0.25		[#]2.72 ± 0.71	
Δm	NA		[#]2.15 ± 0.51		[#]4.21 ± 0.72	

PACAP selectively increases mean quantal content. Results depict mean quantal size (i) and quantal content (m) determinations from spontaneous EPSCs, evoked EPSCs, and transmission failures. Only those cases where i and m were determined for both PACAP- and control (sham-treated) neurons (n) in the same experiments are presented. Values of quantal size and content for PACAP-treated neurons normalized to averages from control neurons in the same experiments are indicated by i^* and m^*, respectively. Slopes of quantal content values from PACAP-treated neurons plotted *versus* corresponding values from control neurons in the same experiments ($\Delta m_{PACAP} / \Delta m_{Control}$) are indicated by Δm. The [#] symbol signifies a significant difference ($p < 0.05$), determined by t-test (i, i^*, m, m^*) or F-test (Δm), in the indicated parameter between PACAP-treated and control neurons. The same quantal size values apply for both evoked and failure (--) assays.

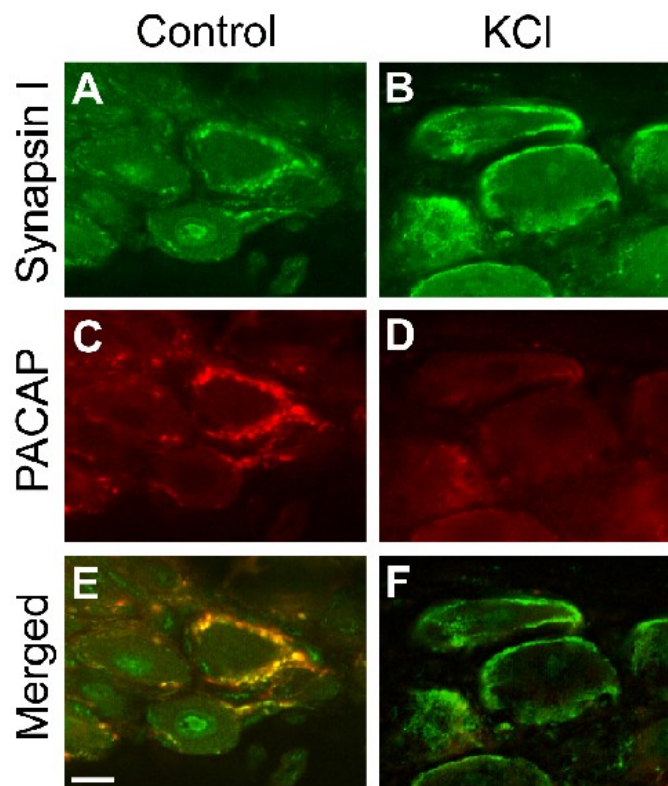Figure 1   Pugh, Jayakar & Margiotta 2009

Figure 2.   Pugh, Jayakar & Margiotta, 2009

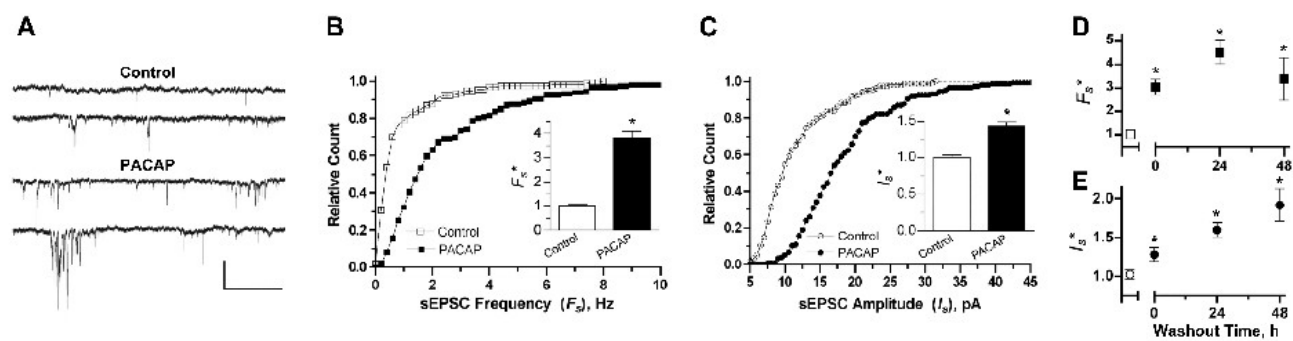Figure 3.   Pugh, Jayakar & Margiotta, 2009
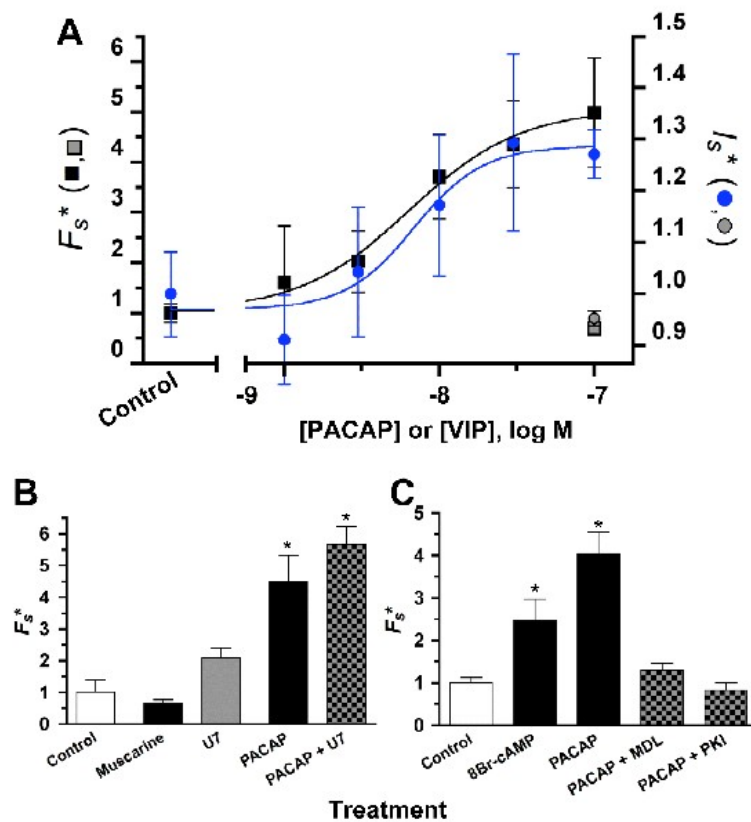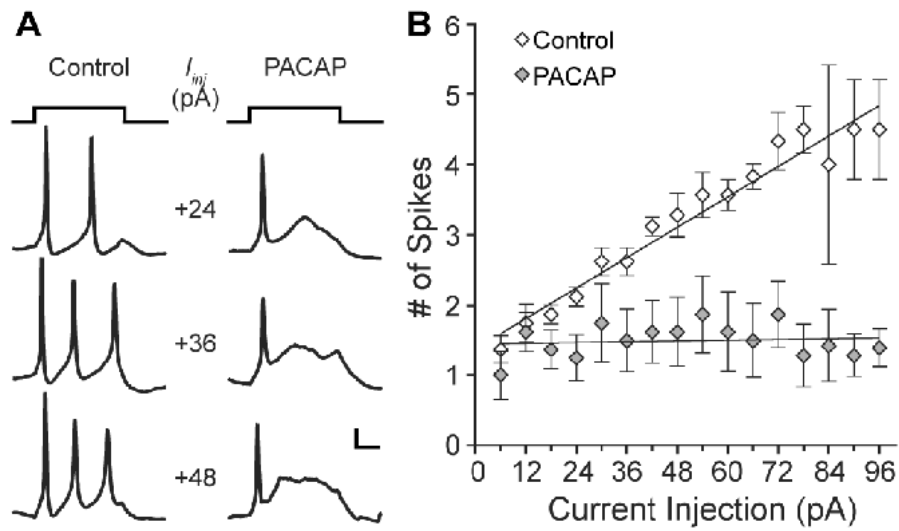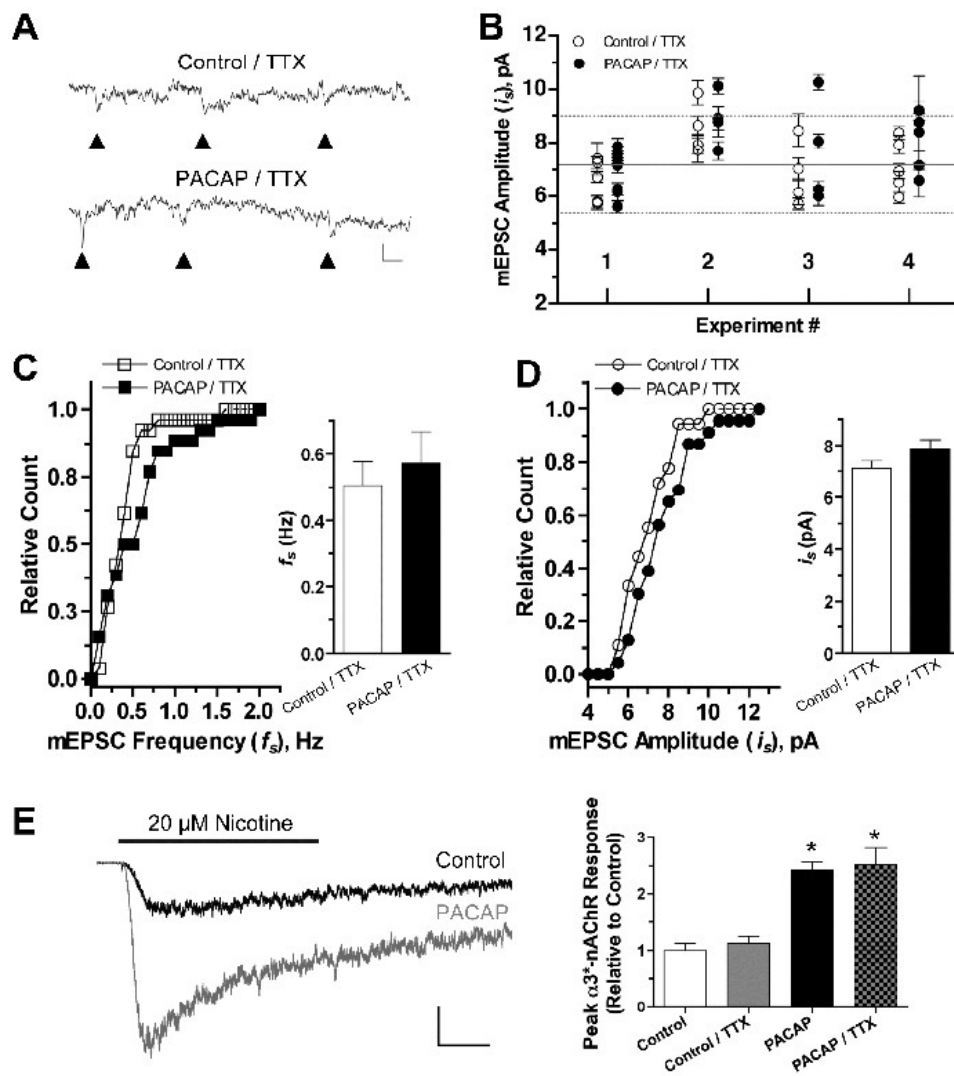
Figure 4

Pugh, Jayakar and Margiotta 2009

Figure 5.   Pugh, Jayakar & Margiotta, 2009
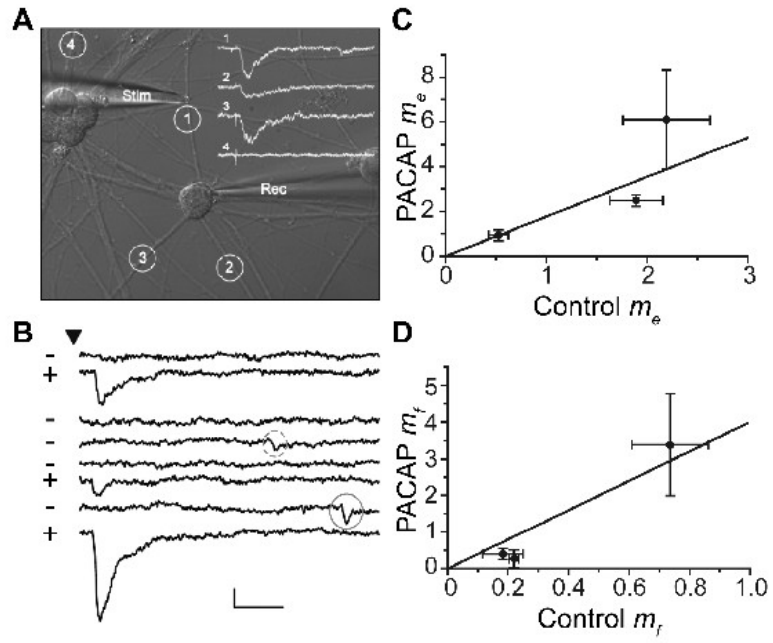
Figure 6.   Pugh, Jayakar, & Margiotta, 2009

Figure 7.   Pugh, Jayakar & Margiotta, 2009